LIP-STUDENTS-24-03

Improving Neutrino Detection at the Pierre Auger Observatory through Vertical Events

Beatriz Carvalho[1,a] and David Dias[1,b]

[1] *Instituto Superior Técnico, Lisboa, Portugal*

Project supervisors: Prof. Ruben Conceição and Pedro Costa

October 7, 2024

Abstract. With the continuous rise in popularity of the multi-messenger approach to event detection, neutrino detection also becomes more important due to the unique information these particles provide. This work follows in the footsteps of previous work in improving this detection at the Pierre Auger Observatory, attempting to distinguish the main source of background, protons, i.e. cosmic rays from UHE neutrinos. It is shown that the depth of the shower maximum, $X_{\max}$, can be explored to further improve Auger sensitivity to UHE neutrinos.

Keywords: UHE Neutrinos, $X_{\max}$, S_{em} and S_{μ}, Extensive air showers, Event classes

1 Introduction

1.1 Extensive Air Showers

When a highly energetic particle enters the atmosphere an extensive air shower is formed. These are typically created by charged particles interacting with the air [1]. Upon collision, hadronic interactions will lead to the formation of pions and other hadronic particles. Charged pions can propagate these interactions, creating an hadronic cascade while others might simply decay, typically into muons (and muon neutrinos) through the weak interaction, leading to the formation of a muonic cascade. Since muons have low cross-sections, they will typically reach the ground and consequently, the detector, giving us a reliable measure on the hadronic signal. On the other hand, the neutral pions tend to decay into two photons, which, at such high energies, will create electron-positron pairs, which in turn, radiate photons through bremsstrahlung creating an electromagnetic cascade.

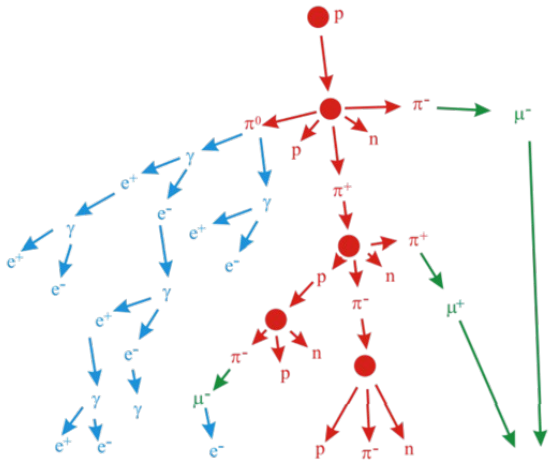

Figure 1. Schematic example of a typical hadronic shower. In blue we see the electromagnetic cascade, in red its hadronic counterpart and, in green, the muonic cascade.

It is worth noting that the depth travelled by these cascades before being fully contained by the atmosphere greatly varies between cascade types. Electromagnetic (e.m.) showers are characterised by their radiation length while hadronic showers, far more complex, are determined by the mean free path between inelastic collisions, which is usually much greater than the e.m. cascade's radiation length. This implies that an electromagnetic shower can be contained within a smaller depth than the hadronic variant. One of the most common charged particles entering our atmosphere are protons. They will typically interact in the top of the atmosphere, which isn't the case if the primary particle has a very low cross-section, such as a neutrino. Neutrinos can weakly interact with the Earth's atmosphere and create a similar cascade to a proton's. The hadrons which it collides into form the hadronic cascade, while the lepton resulting from the interaction might radiate and form its electromagnetic cascade. The big difference here is the height at which the first interaction takes place, neutrinos interact very little, so the probabilities of

[a] e-mail: beacarvalhogoncalves@gmail.com
[b] e-mail: david.fialho.dias@tecnico.ulisboa.pt

interacting close to the ground or at the top of the atmosphere are very similar, and close to zero, unlike the proton.

1.2 Pierre Auger Observatory and Neutrinos

The Pierre Auger Observatory, located in Argentina at around 1400 m of altitude, was built to detect UHECR (ultra-high energy cosmic rays, energies above 10^{18} eV) [2]. Its main detection methods are an array of 1600 water Cherenkov detectors (WCDs), spanning an area of 3000 km^2, each spaced 1.5 km apart, which detect particles through their interaction with the water placed in surface detector tanks, and the fluorescence detectors (FDs) which capture the ultraviolet light emitted by the extensive air showers.

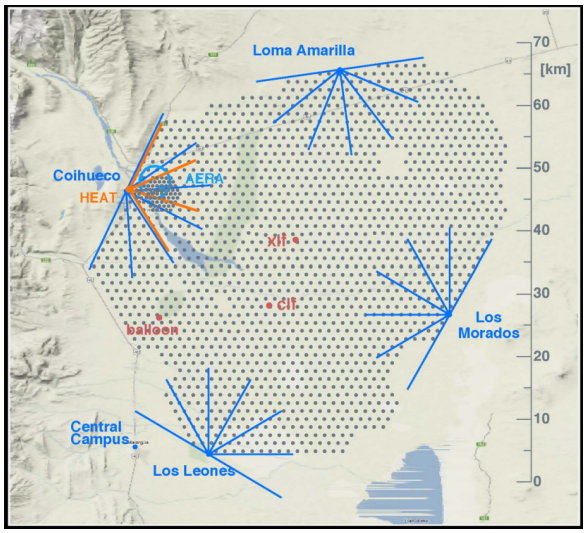

Figure 2. Pierre Auger Observatory, each black dot represents a station of the surface array while the blue lines illustrate the location and direction of detection of the fluorescence detectors.

The WCDs collect the Cherenkov light from incoming particles and register it as a signal. Within the simulations it is possible to separate this signal into an electromagnetic signal (S_{em}) or a muonic signal (S_μ), corresponding to a total registered signal from the collection of light across the surface detector array, associated with the electromagnetic or the muonic/hadronic cascades, respectively. Currently, the Auger collaboration is attempting to achieve this with the experimental data using Machine Learning techniques and the information which will be available once all scintillating surface detectors (SSDs) are installed [3]. The FDs, while having a lower duty-cycle (the fraction of time during which the detector is active), allow us to obtain the longitudinal profile of the shower, adding onto the information obtained by the WCDs.

Previous neutrino searches focused on the signals registered by the WCDs. They looked for very inclined showers ($\theta \in [60^\circ, 88^\circ]$) without much S_{em} since showers at large angles typically only have muonic signal. This is simply because the depth in the atmosphere that the inclined shower has to travel to reach the detector is larger, which for protons interacting at the top of the atmosphere means the electromagnetic cascade won't reach the ground, only the muons will. This isn't the case for neutrinos, since they might interact closer to the detector, and being registered as a "young" shower, i.e. the e.m. component hasn't been absorbed yet. The most common technique currently in use, however, are the "Earth-skimming neutrinos", consisting of detection of events with ground level or slightly below reconstructed direction, implying a particle crossed massive distances, possibly through the Earth, to reach the detector, implying a neutrino origin to these events [4].

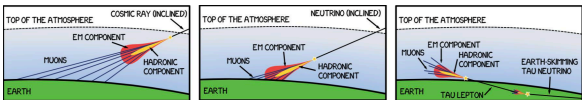

Figure 3. Neutrino detection methods used at Pierre Auger Observatory. The e.m. component reaches the ground if the very inclined shower is of neutrino origin (two images on the left, comparison between cosmic rays and neutrinos). Most common method visible on the right, the "Earth-skimming neutrino", seen in this example reaching the detector from slightly below ground level.

The surging interest in neutrinos comes as a consequence of the attention gathered around the topic of multi-messenger astronomy. This strategy consists in using different "messengers" from a single event in order to acquire more information about it. These messengers can be gamma-rays (light), cosmic rays (charged particles), gravitational waves and neutrinos. Each can tell us something unique about the event being studied, so, combining them, when possible, is the best strategy. Neutrinos in particular are very useful, as they are not deflected by galactic and inter-galactic magnetic fields, all while crossing straight through any object in their path, which makes them ideal in determining the direction of a source. The Pierre Auger Observatory has 17 years of shower data stored so having a method which could distinguish between its main focus, i.e. cosmic rays, and neutrinos could help boost our knowledge on past events, as well as getting a "new" neutrino detector without the effort of building one, ensuring a better preparation for future remarkable events.

2 Previous Results

2.1 Differential neutrino flux

The GZK effect predicts an upper limit on the energy of cosmic rays, assuming these are protons, it indicates that there's a certain energy at which the proton should interact with cosmic microwave background photons and hit the Δ resonance, splitting the energy between proton and the newly produced pion ($p + \lambda_{\mathrm{CMB}} \rightarrow \Delta^+ \rightarrow p + \pi^0$). These UHE protons should also be able to interact with photons at the source and produce neutrons and charged pions, which can decay into neutrinos and leptons, forming UHE neutrinos. Despite this, only HE neutrinos have

ever been observed, imposing limits on the flux of these particles at these energies. The equation for the differential neutrino flux is:

$$E^2\frac{dN}{dE} = E^2\left(2\pi A\Delta E\Delta t\int\int\frac{\sigma}{m}\sin\theta\cos\theta\,\epsilon(E,D,\theta)d\theta dD\right)^{-1} \quad (1)$$

Where $A = 2.97\times10^3$ km^2 is the area occupied by the observatory, $\Delta\log_{10}(E/\text{eV}) = 1$, $\Delta t = 17$ years is the total operating time of the observatory, $E = 5\times10^8$ GeV, m = 0.938 GeV is the nucleon mass (taken to be the proton mass), $\epsilon(E,D,\theta)$ is the array's discrimination efficiency and D is the grammage (thickness of atmosphere between the point of neutrino's first interaction and the detector array, in g cm^{-2}). Determining an upper limit on the UHE neutrino differential flux limit can be achieved if we know the array's efficiency at distinguishing neutrino from proton induced events [5].

2.2 New neutrino detection strategy

The very inclined shower detection method has one major issue: it restricts our coverage of the sky to a very small band, a problem the inclusion of vertical showers (θ<60º) would fix, but doing so is not as easy. Since the total atmospheric depth is lower at smaller angles, proton induced showers still retain an electromagnetic signal at detector level, making them very similar to neutrino ones. A method recently introduced consists in looking for the Fisher discriminant which best separates the neutrino data from its background, the protons. To this end, shower data was simulated in CORSIKA, while the detector's response was emulated with Auger OFFLINE.

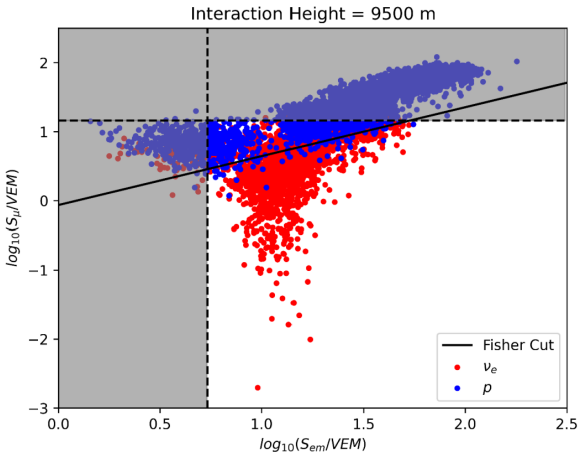

Figure 4. S_{em} vs S_μ example for a fixed interaction height of 9500 m. In blue we see the simulated 10^{18} (left) and 10^{19} (right) eV proton simulations and in red the 10^{18} eV electron neutrino simulations. A Fisher cut (black line) maximizing separation between samples is observable, as well as the signal cuts (grey area) applied.

A new method to distinguish neutrino events from cosmic-ray events, based on the signals from the electromagnetic shower component (S_{em}) and the muonic component (S_μ), was proposed in [6]. By applying a simple Fisher discriminant analysis on the parameter space defined by these two variables, it is possible to fit the tail of the proton distribution and identify a Fisher value corresponding to a desired background rejection factor, or threshold. This way, we can find the Fisher cut which rejects the most amount of protons possible. After this step the data points are split into grammage bins and the efficiency in each bin is extracted. The efficiency here is simply the ratio between neutrino points below the Fisher cut and the total simulated neutrino events. It is then possible to interpolate these efficiencies for each grammage and use this interpolation to integrate in efficiency as shown in eq. 1. Since all simulations are done with $\theta = 38$º the angular integration becomes trivial, only needing to consider the chosen zenith angle bin, and a differential neutrino flux is obtained.

2.3 Muon neutrino

This procedure was first used to determine the differential flux of the electron neutrino, but it can be applied to the muon neutrino if one considers that at these energies, the muon produced in the scattering with the atmosphere will have enough energy to radiate through bremsstrahlung (critical energy, i.e. minimum energy for bremsstrahlung radiation is around 3 TeV), just like the electron, despite its critical energy being several orders of magnitude higher. An electromagnetic cascade, similar to the electron's, should be formed, so the same analysis process can be applied here. Muon neutrinos exhibit lower efficiencies than electron neutrinos since there is a bigger overlap between muon neutrino points and proton ones than in the electron's case, as seen below.

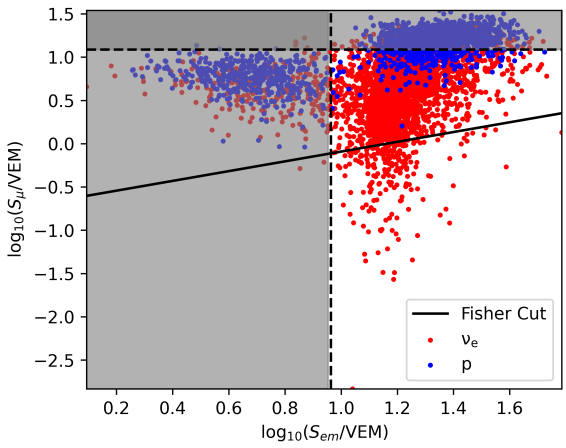

Figure 5. S_{em} vs S_μ for electron neutrino for a 10^8 to 10^9 GeV bin and 140º to 145º zenith angle bin.

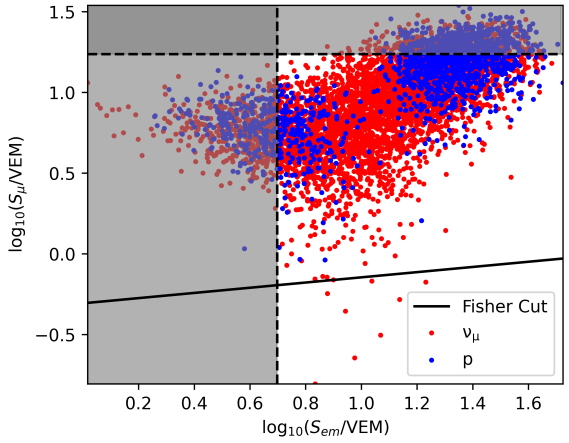

Figure 6. S_{em} vs S_{μ} for muon neutrino for a 10^8 to 10^9 GeV bin and 140º to 145º zenith angle bin. A bigger overlap than in the electron neutrino's case is observable

Below are the flux results obtained:

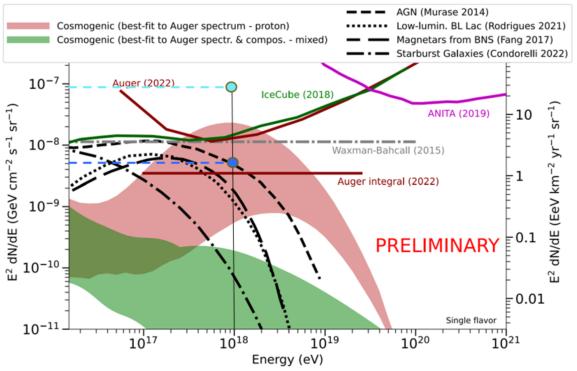

Figure 7. Differential flux results obtained for the electron (dark blue) and muon (light blue) neutrinos using an energy bin of $[10^{18}, 10^{19}]$ eV and angle bin of [35º, 40º] at a 10^{-4} threshold.

The neutrino differential fluxes obtained on this previous work were:

- $\nu_e = 4.09 \times 10^{-9}$ GeV cm^{-2} s^{-1} sr^{-1}
- $\nu_{\mu} = 8.68 \times 10^{-8}$ GeV cm^{-2} s^{-1} sr^{-1}

Despite the success at distinguishing neutrino from proton induced events, these limits, in particular the less efficient muon neutrinos, could be achieved at a lower threshold and improved if we used another variable with great distinction power. The chosen variable was X_{max} , the longitudinal depth at which a shower reaches its maximum number of particles.

3 Internship

3.1 A new approach: X_{max}

The main goal of the internship was to find out if X_{max} is a good measure to distinguish proton events from muon neutrino events. In order to do that, it is necessary to fit each longitudinal profile.

To fit each profile the Gaisser-Hillas function, shown below, was used.

$$N' = \left(1 + \frac{RX'}{L}\right)^{R^{-2}} \exp\left(-\frac{X'}{LR}\right) \tag{2}$$

with $N' = N/N_{max}$, the fraction of particles in relation to the maximum number of particles and $X' = X - X_{\text{max}}$ the depth of each stage of shower development shifted by X_{max} (where the depth at which the simulated point had the highest number of particles was taken as an initial guess, to be improved upon using the fit above).

Below the different fit classes can be seen. From the first class the X_{max} can be extracted.

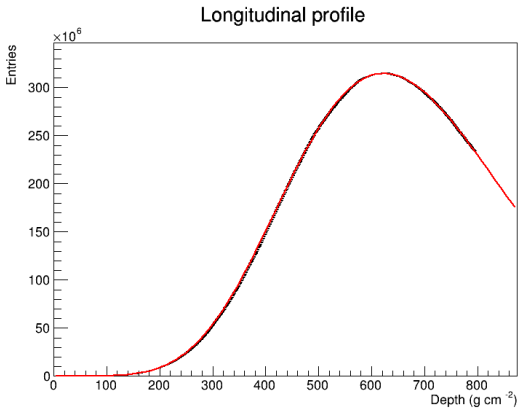

Figure 8. Example of a Class A event.

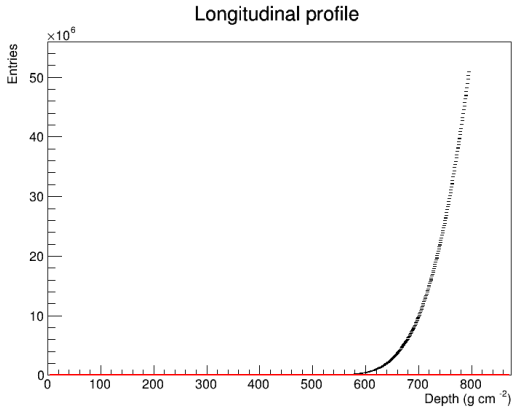

Figure 9. Example of a Class 1 event.

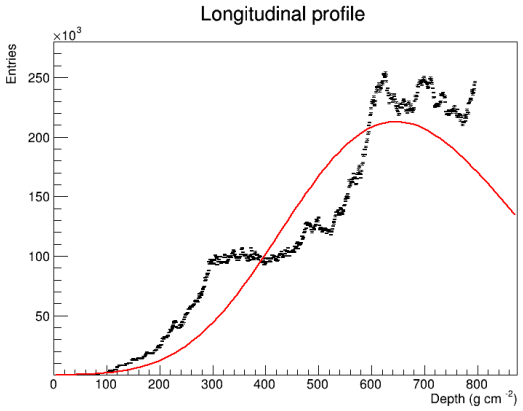

Figure 10. Example of a Class 2 event.

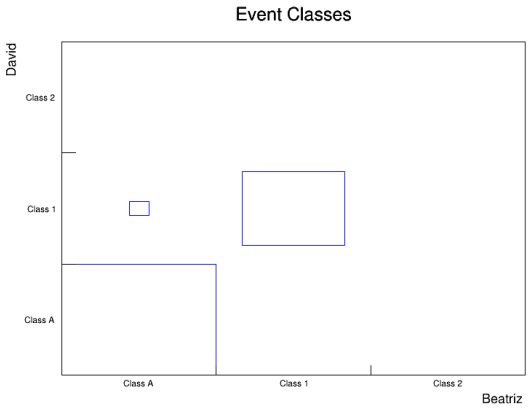

Figure 11. Correlation for proton events.

3.2 Anomalous events

The problem is that not every longitudinal profile can be adequately fitted to a Gaisser-Hillas function, leading to the definition of different types of profiles, as seen in figures 8, 9 and 10. The $X_{\max}$ is only correctly extracted from Class A, since Class 1 does not reach a peak, and therefore it's not possible to know with certainty where it would be, and Class 2 reaches 2 peak zones, so it's also not possible to determine the $X_{\max}$. For these reasons, this research is based solely on Class A events.

In Class A, Fig. 8, the fit, in red, is done correctly and is aligned with the data, in black. In Class 1, Fig. 9, the fitting process failed because the algorithm could not detect a peak. Class 2, Fig. 10, is characterised by multiple peaks, so the fit can detect a peak, but is done incorrectly, not aligned with the data.

3.3 Classification criteria

To automatically classify the events, different approaches were used. The first one focused on the number of entries, by classifying all events with a value below one million as Class 2, initially. Then separated the events based on the presence of a peak. Since there were still some misclassifications in the Class 2 events, they were analyzed again and divided based on the number of peaks. The second approach focused on identifying exponentials by checking if the data points were continuously increasing, with a small tolerance, and then analyse the number of peaks. Of course, different criteria lead to different results, so the figures 11 and 12 show how many events the approaches agreed on, for both types.

The majority of the events were equally classified by the two methods, as represented by the size of the square.

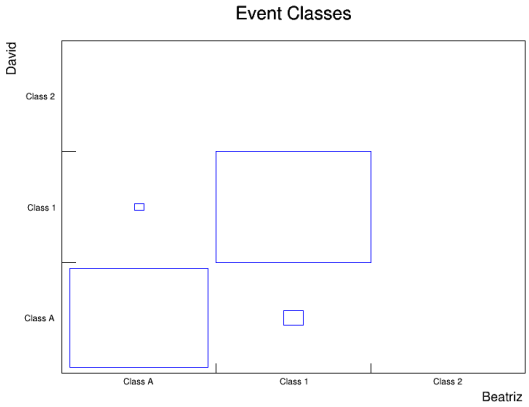

Figure 12. Correlation for neutrino events.

The number of Class 2 events is so low compared to the other classes that they're not shown in the figure, although they exist.

3.4 Classification criteria and Problematic cases

The next figures are examples of the two methods disagreeing. They both belong to Class 2, but had similarities with the others.

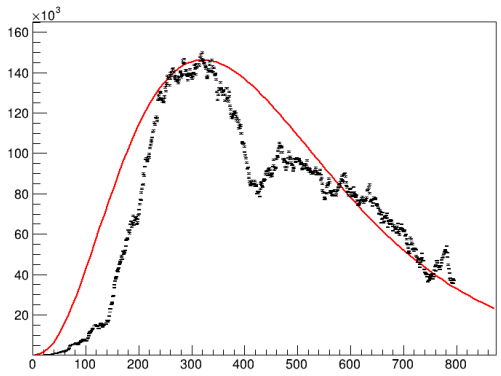

Figure 13. Class 2 event, first classified as Class A.

This misclassification was due to the fit resembling a gaussian function. However, the points clearly show multiple peaks, making the event inappropriate to use as Class A.

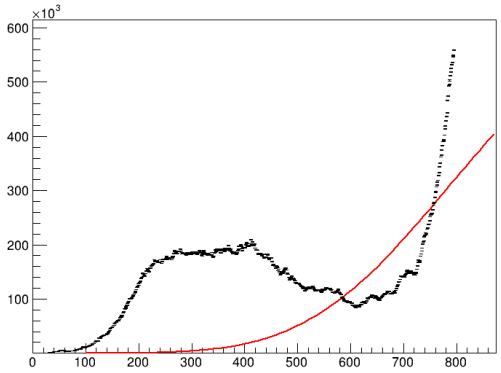

Figure 14. Class 2 event, first classified as Class 1.

This next misclassification was due to the end of the points resembling an exponential. However, that would create a second peak, making it belong to Class 2.

3.5 A combined approach

After looking through the failed classifications the methods were combined to reach maximum accuracy, first separating the events based on the number of entries, which allowed different tolerances for counting peaks. Also, the Class 1 events were determined based on the resemblance to an exponential. This method reached the following distribution of events per class.

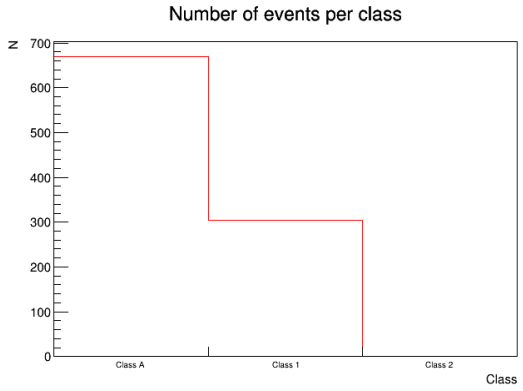

Figure 15. Class distribution for proton events.

The majority of the events in Fig. 15 were classified as Class A. However, the events from Class 1 are quite similar, just not reaching a peak yet.

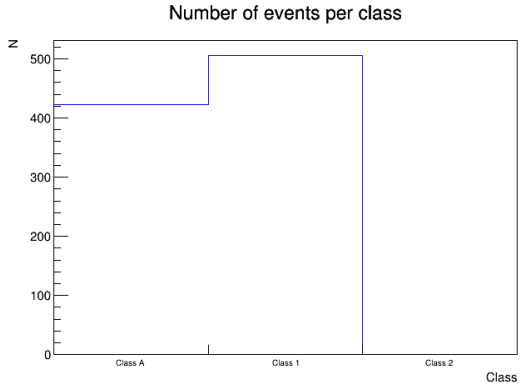

Figure 16. Class distribution for muon neutrino events.

The majority of the events in Fig. 16 were classified as Class 1, with the Class A events next. Once again, the number of events from Class 2 is so low in comparison that they're not represented.

4 Results

The distributions of the X_{max} for both events are not as distinguishable as expected, making the bigger range in depth for the muon neutrino events the only relevant difference.

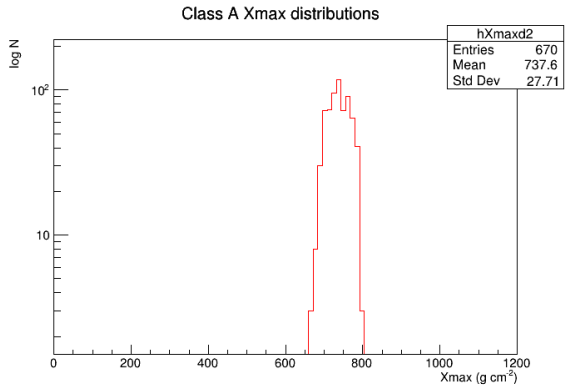

Figure 17. $X_{\max}$ distribution for proton events, with a range of 650 to 800 g cm^{-2}.

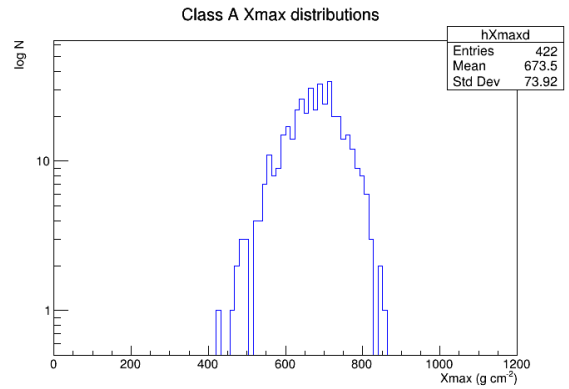

Figure 18. $X_{\max}$ distribution for muon neutrino events, with a range of 420 to 860 g cm^{-2}.

With a robust classification method in hand, the next step was attempting to understand if there truly was a correlation between $X_{\max}$ and S_{em} or S_{μ}, which could be used to further improve separation between protons and neutrino simulations, consequently increasing the neutrino detection efficiency and lower the flux limits at even more stringent thresholds.

The plots below compare the $X_{\max}$, when reconstructable, i.e. when event falls into class A, to S_{em} and S_{μ}, as well as, the class 1 events, from which we only know their $X_{\max}$ is above the ground limit.

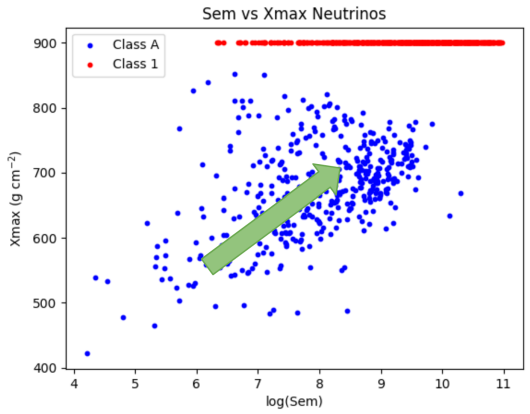

Figure 19. S_{em} vs $X_{\max}$ for muon neutrino.

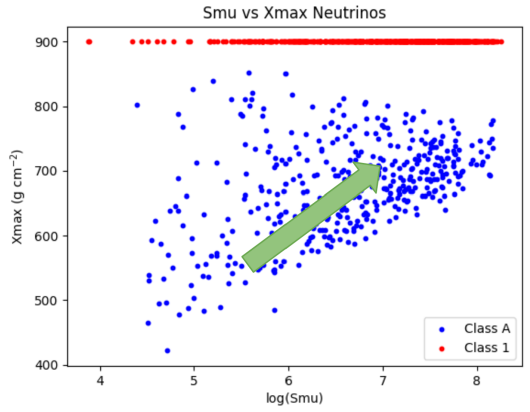

Figure 20. S_{μ} vs $X_{\max}$ for muon neutrino.

A correlation between the studied variables can be seen, implying the possibility of using $X_{\max}$ as a discrimination factor as was hoped.

5 Conclusions

This work followed a new strategy based on electromagnetic and muonic signal at the ground to detect "vertical" ($\theta < 60^{\circ}$) showers and showed that the depth of the shower maximum can be explored to further improve Auger sensitivity to UHE neutrinos.

Acknowledgements

We'd like to thank our supervisors, Prof. Ruben Conceição and Pedro Costa for the all the support and guidance given during this internship, as well as LIP for this amazing opportunity to work in and experience scientific research alongside experts.

References

[1] R. Engel, D. Heck, T. Pierog, Ann. Rev. Nucl. Part. Sci. **61**, 467 (2011)

[2] A. Aab et al. (Pierre Auger), Nucl. Instrum. Meth. A **798**, 172 (2015), 1502.01323

[3] A. Aab et al. (Pierre Auger), JINST **16**, P07016 (2021), 2103.11983

[4] J. Abraham et al. (Pierre Auger), Phys. Rev. Lett. **100**, 211101 (2008), 0712.1909

[5] A. Aab et al. (Pierre Auger), Phys. Rev. D **91**, 092008 (2015), 1504.05397

[6] J. Alvarez-Muñiz, R. Conceição, P.J. Costa, M. Pimenta, B. Tomé, Phys. Rev. D **106**, 102001 (2022), 2208.11072